Mem. S.A.It. Vol. 81, 604

Memorie della

Chromosphere of active regions on the Sun

F. Kneer

Institut für Astrophysik, Friedrich-Hund-Platz 1, D-37077 Göttingen, Germany
e-mail: kneer@astro.physik.uni-goettingen.de

Abstract. The first part of this contribution deals with the chromosphere of sunspots. The models of umbrae give strongly self-reversed Ca H and K line cores. Much 'macro-turbulent' broadening is needed to fit the modeled line profiles to the observations. Thus, observed dynamics in sunspot chromospheres are discussed. In the second part, the chromsphere of plages is treated. We start with the relation of K emission vs. average magnetic field strength and continue with chromospheric models. Since chromospheres are most easily observed in Hα, various simplifications for the interpretation of this line, including the cloud model, are discussed and results are given. Dynamic phenomena in plages, such as moustaches and magneto-atmospheric waves along fibrils, will be shown. Ideas about heating mechanisms of active chromspheres will be mentioned.

Key words. Sun: activity – Sun: chromosphere

1. Introduction

Research into the chromosphere of active regions on the Sun is exciting. Thanks to our proximity to the Sun we can study activity structures with their magical appearance in detail. The often violent processes are far beyond the feasibility of terrestrial laboratories. They have astonished researchers for more than a century. Solar activity convinces the astrophysical community that solar physics is important. It fascinates the public, interested laymen and politicians, who allow us to study the Sun to understand the environment of Earth and beyond, the Sun itself and the stars. I myself remember very well how my late director, Karl-Otto Kiepenheuer, could captivate state presidents and kings with his charming and exciting stories about the Sun, especially the active Sun.

Send offprint requests to: F. Kneer

Research into the active chromosphere is a demanding task. This part of the solar atmosphere owes its complexity to the magnetic fields it harbours. The field strengths vary from few tens of Gauss in weak plages to kilo-Gauss in sunspots. While reacting to convective motions below the photosphere, they dominate the dynamics in the chromosphere. The fields can produce rapid structural changes on time scales of a second and shorter. Thus, to follow such processes, the observations have to be performed at very short cadences, often too short for today's instrumental facilities.

Also the theoretical interpretation of the observations is most challenging. The magnetic field in a conducting fluid adds to the gas pressure and gravity a multitude of further influences: magnetic pressure and tension, waves and instabilities, reconnection with release of large amounts of magnetic energy.

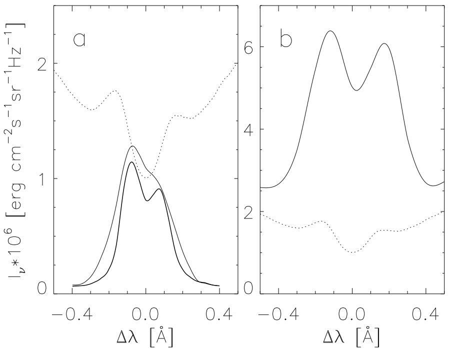

Fig. 1. Central part of Ca II K line. **(a):** quiet Sun (dotted) from Fourier Transform Spectrometer Atlas (Brault & Neckel, quoted by Neckel 1999), from sunspot umbra (thin solid) and from model (thick solid), latter two after Lites & Skumanich (1982). The model profile is convolved with a Gaussian corresponding to a 'macro-turbulence' of 5 km s^{-1}. **(b):** quiet-Sun K line (dotted) and from a plage (after Shine & Linsky 1972). Note the different scales in panels (a) and (b).

Consequently, because of the complexity of the chromosphere of active regions, this contribution can only *touch* on few topics. First, I shall deal with the chromosphere of sunspot umbrae, which also exhibit emission in some spectral lines. We discuss their modelling and the dynamic phenomena observed in umbrae. Second, I shall expand on the chromosphere of plages. Studies of their magnetic flux density (here synonymously denoted as field strength with units Mx cm^{-2} or G) are numerous. A part of this section will be devoted to observations and interpretation of the hydrogen Balmer α line (Hα), to its brightness in plages, and to some of the dynamics seen in Hα. Also mechanisms for the supply of the chromosphere of plages with energy will be mentioned.

2. Chromosphere of sunspot umbrae

2.1. Emission in chromospheric lines

Sunspot umbrae show emission cores in chromospheric lines, such as Ca II H and K, Mg II h and k, and in many more UV lines, e.g. in the hydrogen Ly series. Figure 1a depicts the core of an umbral Ca K line, observed with the OSO 8 satellite by Lites & Skumanich (1982), in comparison with the quiet Sun profile. The central part of the umbral K line is as bright as the quiet Sun profile and *does not* exhibit a self-reversal. For further use below, Fig. 1b gives the core of the K profile from a medium bright plage. This has 3–4 times stronger emission than the quiet Sun K line.

The K to H, or k to h, intensity ratio is an important measure for modelling umbral chromospheres. An optically thin emission, as the pure emission cores suggest, would give

$$I_K/I_H = f_K/f_H = 2\,, \qquad (1)$$

with oscillator strengths $f_{H,K}$. However, all observations give a lower ratio. Especially Turova & Grigoryeva (2000) obtain from their detailed study $I_K/I_H = 1.14$ on average.

2.2. Temperature models of sunspots

One of the first attempts to model umbral chromospheres was undertaken by Kneer & Mattig (1978). Two of their models are reproduced in Fig. 2. To avoid self-reversals, a thin chromospheric model was tested which gives an intensity ratio I_K/I_H much larger than observed. Thick models, resulting in the correct ratio, inevitably give self-reversals, which had to be smoothed out with a 'macro-turbulence' corresponding to 5 km s^{-1}. Beebe et al. (1982) arrived at the same conclusion.

The umbra model by Lites & Skumanich (1982) was based on observations with the OSO 8 satellite. It is also shown in Fig. 2. This model contains a chromospheric temperature plateau required for correct Mg h and k intensities. Again, a 'macro-turbulence' with 5 km s^{-1} was applied. The asymmetry of the profile is produced by a systematic down-flow whose amplitude decreases with depth. The associated enthalpy flow would be a source of energy for chromospheric heating.

Remarkably, the umbral K and H emissions follow the Wilson-Bappu relation (Mattig & Kneer 1981). Besides, cool stars, e.g. ε Eri (K2 V), show very similar Ca H and K emission with little self-reversal, if at all (Linsky et al. 1979). Thus, the shape of the emission cores does not reflect any special

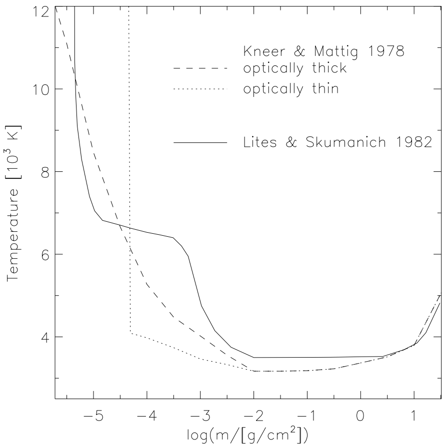

Fig. 2. Run of temperature with column mass density *m* for various umbra models.

heating mechanism caused by the strong umbral magnetic field.

2.3. Dynamics in sunspots

As it holds for any chromosphere, dynamic processes have to occur in umbral chromospheres for the energy transport and energy balance. The umbral flashes were detected in Ca K by Beckers & Tallant (1969) and studied by Wittmann (1969). They are of small scale and quasi-periodic with periods of 140–190 s. Turova et al. (1983), in their systematic work, present an impressive picture of the periodic brightening and asymmetry of the K line core.

Oscillations in Hα Dopplergrams in sunspots were found by Giovanelli (1972, see his Fig. 2). The oscillations have the same period and are thus apparently of the same nature, as the K line flashes.

Waves in umbrae were investigated theoretically already early, among others by Musman (1965). He studied the generation of Alfvén waves in a subphotospheric overstable layer. Uchida & Sakurai (1975) treated umbral oscillations as Alfvén waves trapped between the overstable subphotosphere and the transition region (TR), between the chromosphere and corona. They find low eigenmodes in agreement with the Dopplergrams by Giovanelli (1972).

Zhugzhda et al. (1983) considered slow mode magneto-acoustic waves semi-trapped in the chromospheric cavity, that transmits only waves with suitable period, like a Fabry-Pérot etalon. This differs from the view of Scheuer & Thomas (1981) that the umbral 3-min oscillations are resonant fast modes, excited by the subphotospheric overstable convection. Abdelatif et al. (1983) confirm this latter study by observational evidence that the umbral photosphere contains waves with selected periods too.

The excitation and propagation of waves in umbrae with short periods (10 s) and small spatial extension was studied numerically by Khomenko & Collados (2006). Their results are that fast-mode waves are refracted and reflected downward, while slow-mode waves can reach the chromosphere.

A remarkable detection of sunspot chromospheric dynamics was made by Socas-Navarro et al. (2000). They found in the Ca IR lines periodic (140 s) changes of Stokes *V* profiles, from normal to reversed, strongly asymmetric circular polarisation. They interpret this with a two-component atmospheric structure, a quiet component and an active one with motions of 10 km s^{-1}. These latter form shocks and produce a blue shifted intensity emission, thus reversed circular polarisation. Centeno (2005) confirm the two-channel picture with observations in the He I 10830 Å line. The waves propagate in active channels of diameters $< 1''$. Socas-Navarro et al. (2009), furthermore, see in Ca H filtergrams from Hinode fine structures in umbral flashes with scales down to the resolution limit of $\sim 0\farcs22$. Here we encounter a typical case of loss of understanding because of new, sophisticated observations with high spatial resolution. The picture of 'global' umbral oscillations has to be refined, to say the least.

Simultaneous spectroscopic observations in the Ca II H and He I 10830 regions were recently presented by Felipe et al. (2008). Figure 3 shows a time sequence of H profiles from their data which shows nicely the periodicity and the blue shifted H line cores with enhanced peak intensity. Yet the single profiles do not exhibit self-reversals, despite the good

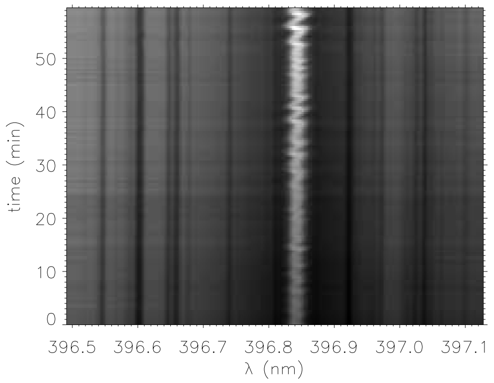

Fig. 3. Temporal evolution of Ca II H in a sunspot umbra; from Felipe et al. (2008).

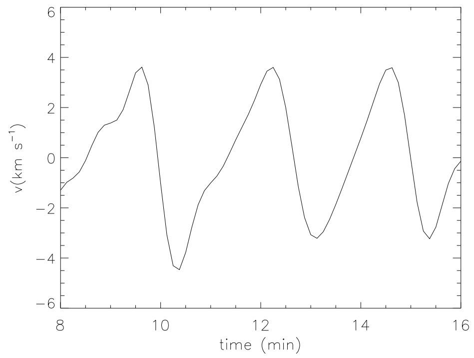

Fig. 4. Detail of velocity time sequence in a sunspot umbra measured in He I 10830 Å showing sawtooth-shaped evolution; from Felipe et al. (2008).

spatial resolution. Figure 4 depicts a part of the associated velocities measured in He I 10830. They form shocks which are a further source of chromospheric heating.

3. Chromosphere of plages

3.1. Emission from plages and relation to magnetic fields

Ca II H, K, and IR line profiles from plages in comparison with quiet Sun profiles were presented, e.g., by Shine & Linsky (1972). An example for the K line core is depicted in Fig. 1. In strong plages, also the Ca IR lines exhibit self-reversed emission cores.

Schrijver et al. (1989) determined the intensity ratio $I_{\rm core}/I_{\rm wing}$ of the K line in solar plages, for certain bandwidths of the core and wing integrations. After subtraction of a minimum ratio (basal K flux) they obtained a linear log-log relation between K emission and average magnetic flux density $< fB >$ in G (f = filling factor, see their Fig. 5)

$$\log(I_{\rm core}/I_{\rm wing}) = 0.6 \log < fB > -2.1\,. \qquad (2)$$

The flux densities are in the range 12–840 G, while the emission ratios vary by a factor of 10.

Subsequently, Schrijver & Harvey (1989) expanded this and similar relations for other chromospheric/coronal emissions, e.g., X ray fluxes, to dependences for Sun-as-a-star measurements and their cycle variation. The goal is to obtain measures of the average magnetic flux density $< f|B| >$ on late-type stars.

Figure 5, from Bello González & Kneer (2008), shows a broadband image from a plage and its line-of-sight (LOS) magnetic field, which is very intermittent at the photospheric level. The average field strength is 30–60 G. From measurements in a plage with the Advanced Stokes Polarimeter and with a Milne-Eddington inversion, Martínez Pillet et al. (1997) found $B \approx 1\,400$ G and $f \approx 0.15$, i.e., an average flux density $< fB > \approx 210$ G.

The strong fields of magnetic flux tubes (I call a magnetic feature even with a mushy cross section a flux tube) at photospheric levels and the average fields in plages have consequences for the field strengths in the chromosphere. We can take $B_0 = 1\,500$ G as the field strength of a flux tube at the base of the photosphere, and an average field strength $B_{\rm av} = 100$ G. From the balance between internal gas pressure $p_{\rm i}$, magnetic pressure $B^2/(8\pi)$, and external gas pressure $p_{\rm ext}$ in hydrostatic equilibrium follows the approximate height dependence

$$B(z) = B_0 \cdot \exp[-z/(2H)]\,. \qquad (3)$$

Take for the pressure scale height $H = 110$ km. The merging height $z_{\rm m}$, where $B(z_{\rm m}) = B_{\rm av}$, is then $z_{\rm m} = 600$ km above the base of the

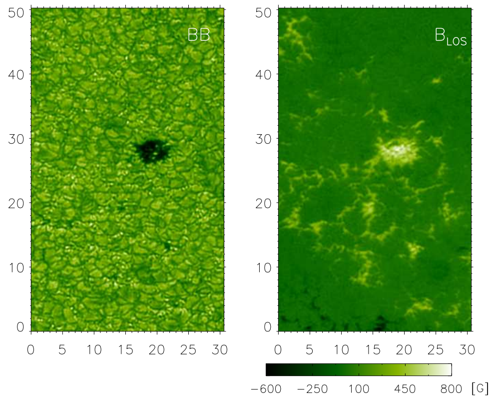

Fig. 5. Weak plage with pore. Left: broadband in 630 nm; right: LOS component of magnetic field; distance of tick marks in arcsec; from Bello González & Kneer (2008).

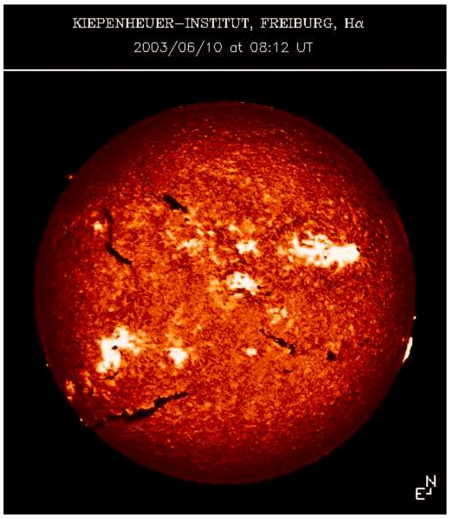

Fig. 6. Full Sun image in Hα line centre, FWHM of filter: 0.5 Å; Hα telescope of Kiepenheuer-Institut at Observatorio del Teide, 10.06.2003.

photosphere. For $B_{\rm av} = 50$ G we arrive at $z_{\rm m} = 750$ km. For strong plages, I expect the magnetic field in the low chromosphere, at 600…1 500 km, to be much more homogeneous than in the quiet Sun, although certainly fluctuating in time and in space.

3.2. Hα line in plages

Hα is a favourite spectral line to observe the Sun, also plages, for four reasons. 1) It is visible to the human eye. 2) It is a strong chromospheric line, since hydrogen is by far the most abundant element in the universe, also on the Sun. 3) It is a broad line, thus filters and spectrographs do not need to have high spectral resolution. 4) One gets a factor 10–100 more photons in one Doppler width of Hα than in, e.g., the H and K lines. But the interpretation of the observations is very difficult because the hydrogen atom is so much dominated by the transitions in the strong Lyα line.

Why is Hα bright in active regions? Figure 6 shows a full Sun image from an epoch when the Sun (still) showed activity. Apart from the filaments and prominences, the latter enhanced by image processing, the bright plages are conspicuous. Their brightness has nothing to do with Doppler shifts. The plages may stay bright for weeks and months.

The problem is that Hα, differently from the collision dominated H and K lines, is photoionisation dominated (Thomas 1965; Mihalas 1970). While the H or K lines can be approximated by radiation transfer in a two-level atom, the bound levels involved in Hα are close to the hydrogen continuum level. The line source function for this two-level plus continuum atom can be written as

$$S_{\rm l} = \frac{\int J_\lambda\, \phi(\lambda)\, {\rm d}\lambda + \varepsilon B_{Te} + \eta B^*}{1 + \varepsilon + \eta}\,, \qquad (4)$$

with integration over the line profile and angle averaged intensity J_λ. The absorption profile $\phi(\lambda)$ is normalised. B_{Te} is the Planck function for the electron temperature, $\varepsilon \approx C_{\rm ul}/A_{\rm ul} = 10^{-6} \ldots 10^{-4}$ gives the ratio of collisional to radiative de-excitation from the 3rd to the 2nd hydrogen level. It can be very small.

In Eq. 4, η and B^* contain the collisional, but mainly radiative transitions from and to the continuum level to the 3rd and 2nd level. They are mainly given by the background radiation fields in the Balmer and Paschen continua, which come from the deep photosphere and are barely influenced by the plage activity. These terms dominate the Hα source, *in the quiet chromosphere*.

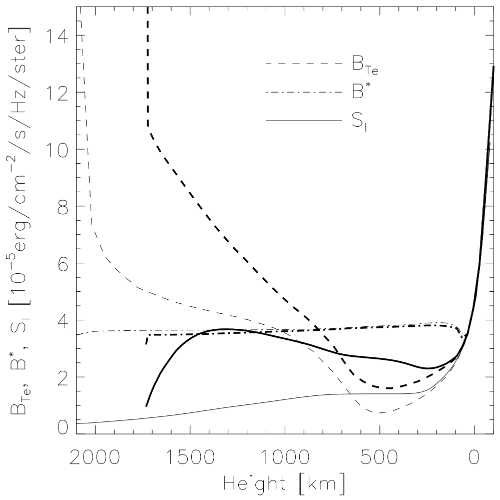

Fig. 7. Height dependence of Planck function for electron temperature, B_{Te}, radiative term B^* in Eq. 4, and line source function S_l; thin: VAL C model (Vernazza et al. 1981); thick: FAL P model (Fontenla et al. 1993).

3.3. Chromospheric plage model

Let us see how Hα comes out from plage models. Figure 7 depicts the height dependence of B_{Te}, B^*, and S_l from two atmospheric models, the average quiet Sun model VAL C (thin curves) and the plage model FAL P (thick).

B^* is almost equal in both models, since the same radiation temperatures in the Balmer and Paschen continua were chosen for both models. But B_{Te} differs considerably in both models, of course, and so does S_l. The height dependence of the terms εB_{Te} and ηB^* is shown in Fig. 8a. Again, the latter does barely differ in the two models, while the former does. The FAL P model is much hotter in the chromosphere than VAL C and has higher electron densities. Thus, in FAL P, the term εB_{Te} in Eq. 4 dominates in the high chromosphere, while it is negligible in VAL C.

The cores of the ensuing Hα profiles are seen in Fig. 8b. The emission in the flanks of Hα from FAL P should be taken *cum grano salis*. The profile calculations were performed with the two-level plus continuum approximation and without partial redistribution. Yet the intensity in the central part of Hα in FAL P

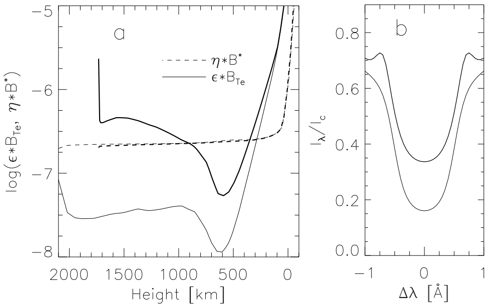

Fig. 8. (a): Terms $\varepsilon \cdot B_{Te}$ and $\eta \cdot B^*$ in Eq. 4 in units of erg cm^{-2} s^{-1} Hz^{-1} ster^{-1} as functions of height; thin: VAL C model, thick: FAL P model. **(b):** resulting Hα profiles.

comes out twice larger than in VAL C, as observed (cf. below). A plot similar as Fig. 7, but with dependence on line-centre optical depth, shows that in FAL P the line minimum of Hα originates partly in the TR.

Figure 7 also points to the heating problem of plages. They are hotter than the quiet Sun from the photosphere to corona. Enhanced radiation from the plage photosphere is needed to account for the variation of the solar irradiation (Wenzler et al. 2005, and references therein). Possibly, the photospheric temperature in plages is heated by the hot walls of magnetic flux tubes, as shown, e.g., by Fabiani Bendicho et al. (1992).

The TR in FAL P is located at a lower height than in VAL C. Hammer (1982) gives the following explanation. The position of the TR is regulated by the coronal heating. From there, the energy is conducted to the TR where most emitters are located. Much/little energy requires high/low density in the TR. Hansteen et al. (2010) argue that the position of the TR is fixed by the runaway of temperature when the chromosphere can not get rid of the energy. Thus more energy supply in the chromosphere moves the TR down too.

3.4. Cloud model and beyond

The cloud model was invented by Beckers (1964) to obtain information on Hα finestructures without the nasty task to solve the 3D radiation transfer problem for the hydrogen atom. The model assumes that a cloud is located high above the atmosphere and does not influence the structure and emission of low layers. Then the contrast $C(\lambda) = [I(\lambda) - I_0(\lambda)]/I_0(\lambda)$ of the cloud becomes

$$C(\lambda) = (S/I_0(\lambda) - 1) \cdot (1 - e^{-\tau(\lambda)}), \qquad (5)$$

with $I(\lambda)$ and $I_0(\lambda)$ the intensities emerging from the cloud and ingoing into the cloud from below, respectively, and S the source function in the cloud assumed constant. E.g. Al et al. (2004) describe how from the contrast profiles the parameters S, optical depth of the cloud at line centre τ_0, the cloud velocity υ_{LOS}, and the Hα Doppler width $\Delta\lambda_{\mathrm{D}}$ in it can be determined by a fitting procedure.

The resulting parameters are typically, with some scatter, $S/I_{\mathrm{c}}{\sim}0.15$ (with I_{c} = continuum intensity), $\tau_0 \sim 1$, $\upsilon_{\mathrm{LOS}} \sim 10$ km s^{-1}, and $\Delta\lambda_{\mathrm{D}} \sim 0.35$ Å (cf., e.g. Sánchez-Andrade Nuño et al. 2008).

Be N_2 the density in the 2nd hydrogen level, L the geometrical thickness of the cloud, and f the Hα oscillator strength, one gets

$$\tau_0 = 1.38 \times 10^{-21} \times (N_2 L)/\Delta\lambda_{\mathrm{D}} . \qquad (6)$$

A deeper account on the cloud model and its recent developments is given in the review by Tziotziou (2007, and references therein).

¿From the width of the cloud structure and assuming a circular cross section of the cloud one obtains from Eq. 6 N_2. With this and the Doppler width and assuming a 'microturbulent' broadening corresponding to 10–15 km s^{-1}, one may derive secondary parameters. For this one uses detailed non-LTE calculations for hydrogen in isolated chromospheric structures. Such calculations were carried out for prominences by Poland et al. (1971) for a wide range of parameters. The comparison with cloud parameters yields typical values for the total hydrogen density $N_{\mathrm{H}} \sim 1.1 \times 10^{11}$ cm^{-3}, for the electron density $N_{\mathrm{e}} \sim 7 \times 10^{10}$ cm^{-3}, and for the temperature $T_{\mathrm{e}} \sim 15\,000$ K. Leenaarts et al. (2010) pointed out that this procedure assumes independence of time, which may not apply in the dynamic chromospheric structures.

The cloud model often fails, because the condition of isolation is not fulfilled, i.e., there is no reaction back on the underlying atmosphere. Therefore, Al et al. (2004) have carried out 2D radiative transfer calculations for Hα in the two-level plus continuum approximation, while the chromospheric structures are assumed embedded in the atmosphere. I summarise the results:

1. A low absorption structure, i.e., a partly evacuated structure, appears brighter than its surrounding. This is caused by the escape of photons from the structure's walls, which is Cannon's (1970) channelling effect.
2. If this partly evacuated structure is located deep in the atmosphere and is very hot, and if on top of it lays normal absorbing gas, it appears bright in the flanks/wings of Hα, but is inconspicuous near line centre. The structure produces a typical moustache profile (see below).
3. A strongly absorbing structure, e.g., a low lying fibril filled with gas, appears *dark*, but shows fibrils next to it that are *brighter* than average all along the Hα profile. This is another case of photon channelling.

van Noort & Rouppe van der Voort (2006) have described rapid temporal evolution of chromospheric structures observed in Hα filtergrams. One of them was a bright blob with proper motion of 140 km s^{-1} (see their Fig. 2). An isolated hot cloud moving with that speed across the solar surface is difficult to conceive. In view of the work of Al et al. (2004), I suggest as an interpretation a chain-like feature of absorbing structures above a bright background that move to and fro, thus giving the impression of a moving bright structure. In the description of their Fig. 3, the authors speak about moving bright features in a loop system. Again, I suggest that it is the dark fibrils/blobs that move, resulting in changing brightness next to them.

3.5. Dynamics in plages

By means of observations obtained and analysed by Sánchez-Andrade Nuño et al. (2008), I now review a few dynamic phenomena in active regions. Figure 9 shows a section of a flar-

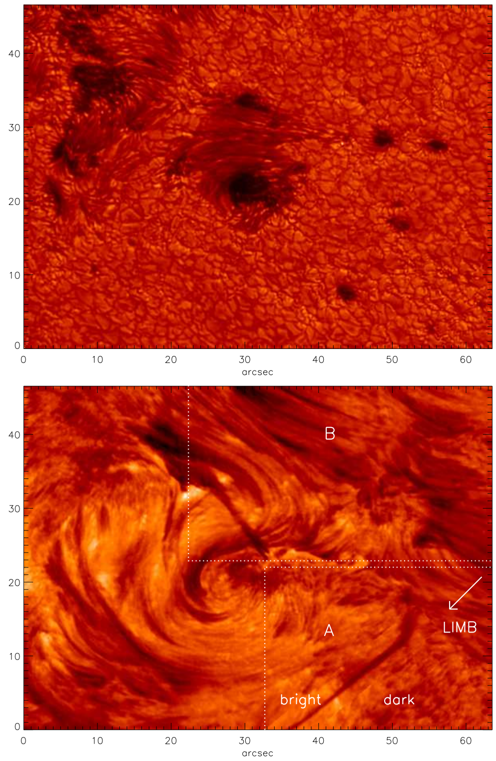

Fig. 9. Section of active region AR 10875 in broadband around 630 nm (upper) and in Hα +0.5 Å off line centre (lower), from Sánchez-Andrade Nuño et al. (2008).

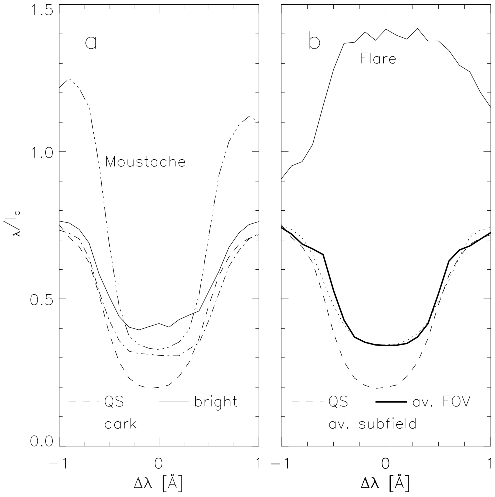

Fig. 10. Several Hα profiles from active region compared with quiet-Sun profile (QS) from an area nearby. Profiles denoted as 'bright' and 'dark' are temporal and $0\farcs33 \times 0\farcs33$ averages from the areas 'bright' and 'dark' in Fig 9, respectively. 'Av. subfield' and 'av. FOV' denote the average profile from region 'A' and from the whole field-of-view (FOV) in the same figure, respectively.

ing active region at a heliocentric angle $\vartheta \approx 36°$. The inner parts of some Hα profiles from this region are depicted and compared to the quiet-Sun profile in Fig. 10a. Note that moustaches can become very bright in the wings of Hα, but are inconspicuous around line centre.

3.5.1. Ellerman bombs/moustaches

Ellerman (1917) himself called these brightenings, best seen in Hα, 'solar hydrogen bombs'. From their appearance in negatives of photographic films, Severny (1956) coined the name 'moustache'. They are small-scale structures with lifetimes of few min. Some authors claim that they possibly live for hours. According to the studies of Bruzek (1967), moustaches occur in developing active regions and in there within mainly around sunspots, but are absent around old, unipolar spots. Denker (1996) gave an account of earlier work on this phenomenon.

Moustaches are bright in the wings of the Balmer lines and are also seen in Ca H and K, but are inconspicuous at line centre of Hα, cf. Figs. 10a and 11. Moustaches are thus a phenomenon of the upper photosphere to lower chromosphere and may be explained by (very) hot gas there, as described in item 2 above, where I discussed embedded Hα structures.

Simultaneous observations of emission at 1600 Å (with TRACE) and in Hα were performed by Qiu et al. (2000). They found two types of moustaches. One type exhibits strong emission and shows a good correlation between UV and Hα, the other comes with weaker emission and little correlation. The authors argue that moustaches are caused by heating in the photosphere. SOHO/MDI, TRACE (195 Å & 1600 Å), and THÉMIS (MSDP & MTR) data were recently used by Pariat et al. (2007) and Berlicki & Heinzel

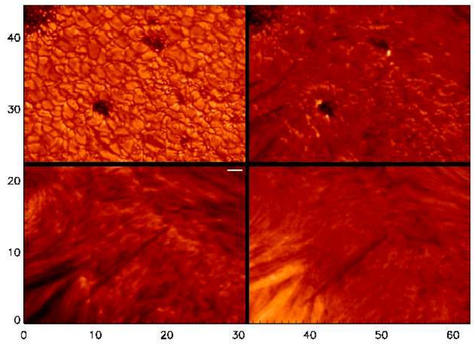

Fig. 11. Snapshot of movie showing Ellerman bombs in Hα, region 'A' of Fig. 9; clockwise from upper left: broadband image in 630 nm, Hα -0.9 Å off line centre with Ellerman bombs close to evolving pores, Dopplergram (difference of intensities at ± 0.5 Å off line centre), Hα -0.5 Å off line centre; length of white bar in lower left panel corresponds to $2''$.

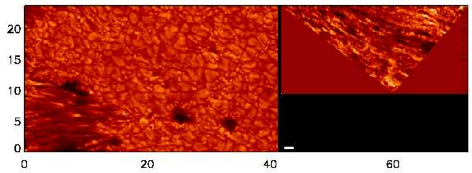

Fig. 12. Snapshot of movie with magneto-acoustic waves seen in Hα, region 'B' of Fig. 9; left: broadband image in 630 nm; right: Dopplergram after high-pass filtering with cutoff period ~ 180 s; length of white bar in right panel corresponds to $2''$.

(2010) to study emerging flux in a developing active region. They find the moustaches located near the magnetic inversion line and suggest heating in low layers by reconnection in a succession of magnetic ΩUΩ... loops, i.e., in a 'sea serpent' topology.

Figure 11 shows a snapshot from a movie of the region 'A' of Fig. 9, lower panel. The image at -0.9 Å off line centre of Hα exhibits moustaches at the borders of the pores. They can become very bright, while very little, if anything at all, is seen at -0.5 Å off line centre or in the broadband image or the Dopplergram. The accompanying movie demonstrates that moustaches live for 2–4 min. Then, nearby, other moustaches appear and disappear, which may give the impression of longevity. In view of the location within an evolving magnetic structure, the reconnection picture at low atmospheric layers appears reasonable.

3.5.2. Magneto-acoustic waves

In region 'B' in the lower panel of Fig. 9, one sees elongated fibrils. They are preferred objects to study magneto-acoustic waves as in Sánchez-Andrade Nuño et al. (2008). The authors subjected the temporal sequence of the data to a high-pass filter to bring out the wave motions otherwise buried among the long lasting flows in the fibrils. Figure 12 shows in its right panel a snapshot of the resulting Dopplergrams. The wave structures are small, $\sim 0\overset{''}{.}5$ thick and only 2–$3''$ along the fibrils. The accompanying movie, with a frame rate of 22 s, suggests that the waves are excited from both sides, at the rooting of the magnetic fields buffeted by the granular motion. From the direction to the limb of the FOV and from the excitation at both ends of the fibrils, we may adopt that, along a large section of the fibrils, the waves propagate parallel to the solar surface and perpendicularly to the LOS.

Figure 13 gives space-time slices of a part of the wave motions from the Hα observations. Periodic repetition is rarely seen. The waves appear to be solitary. One can measure the phase speeds and obtains velocities in the ranges 10–14 km s^{-1} and 23–40 km s^{-1}. The waves often start off with low velocity, close to the sound speed, then speed up to ~ 30 km s^{-1}, and finally disappear, but still in the FOV. The wave train at '1' in Fig. 13 travels for approximately 9 min with ~ 13 km s^{-1}, the waves at '2', '3', and '4' have speeds of 23–30 km s^{-1}.

Sánchez-Andrade Nuño et al. (2008) tried an interpretation with the following considerations. The sound velocity and Alfvén velocity are given, respectively, by

$$c_s^2 = \gamma \frac{p}{\rho} \quad \text{and} \quad \upsilon_A^2 = \frac{B^2}{4\pi\rho}\,. \tag{7}$$

Spruit (1982), from linearisation of the MHD equations of cylindrical flux tubes with

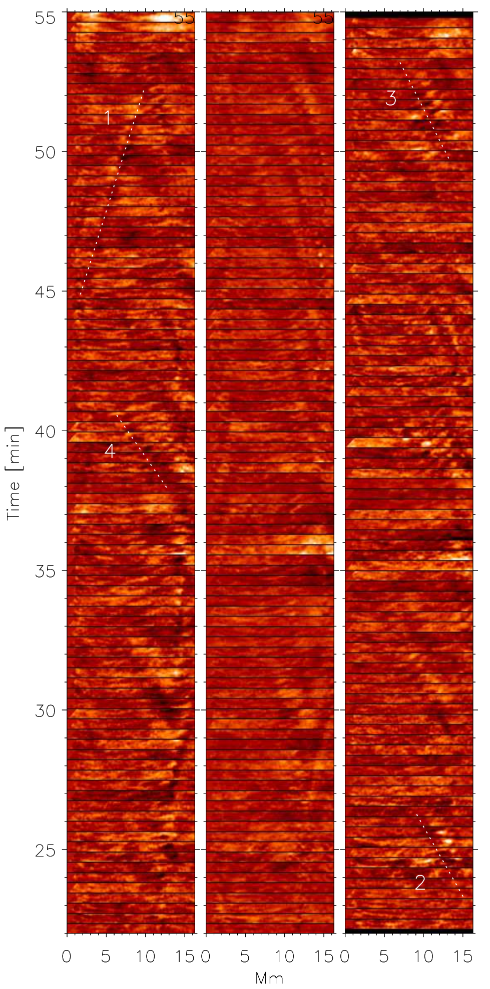

Fig. 13. Space-time slices (16.2 Mm×0.8 Mm, Δt = 22 s, after high-pass filtering) from fibrils in region 'B' of Fig. 9; from left to right: LOS velocity, Hα line centre intensity, and differences $I_{0.5}(t_{i+1}) - I_{0.5}(t_i)$, $I_{0.5}$ = intensity at +0.5 Å off line centre.

density ρ and field strength B, embedded in a medium with $\rho_{\rm ext}$ and $B_{\rm ext}$, gives for the tube speed for longitudinal waves (gas motions along B, the sausage mode)

$$c_{\rm t}^2 = \frac{\upsilon_{\rm A}^2 c_{\rm s}^2}{\upsilon_{\rm A}^2 + c_{\rm s}^2} \, . \tag{8}$$

For $\upsilon_{\rm A} \gg c_{\rm s}$ one has $c_{\rm t} \approx c_{\rm s}$, i.e. propagation with sound speed.

The kink mode (with gas motions perpendicular to B) travels with the phase speed

$$\upsilon_{\rm ph}^2 = \frac{\rho \upsilon_{\rm A}^2 + \rho_{\rm ext} \upsilon_{\rm A,ext}^2}{\rho + \rho_{\rm ext}} = \frac{1}{4\pi} \cdot \frac{B^2 + B_{\rm ext}^2}{\rho + \rho_{\rm ext}} \, . \tag{9}$$

For various combinations of external gas density and field strength one finds

$\upsilon_{\rm ph}^2 = \upsilon_{\rm A}^2$ for $\rho_{\rm ext} = \rho,\ B_{\rm ext} = B$,
$\upsilon_{\rm ph}^2 = \upsilon_{\rm A}^2/2$ for $\rho_{\rm ext} = \rho,\ B_{\rm ext} = 0$, and
$\upsilon_{\rm ph}^2 = 2 \cdot \upsilon_{\rm A}^2$ for $\rho_{\rm ext} = 0,\ B_{\rm ext} = B$.

The observed propagation velocities of the solitary waves with approximately sound speed can be understood, although the large observed LOS gas velocities of 1–2 km s^{-1} perpendicular to the wave propagation are astonishing. Yet, the wave propagation with 25–40 km s^{-1} is difficult to imagine. For any reasonable field strengths and gas densities in the fibrils, the phase velocity of the kink waves should be larger than 100 km s^{-1}, which was not observed. Apparently, the physics of wave propagation in densely packed magnetic inhomogeneities is more complex than the assumption of a single flux tube implies.

3.6. Energy supply

The radiative losses from the chromosphere of plages differ between the various plages. They may vary by a factor of 10 (Schrijver et al. 1989), with lowest values only a bit larger than the losses from the average quiet chromosphere. The latter was calculated by Vernazza et al. (1981) from their VAL C model to $\sim 4.5 \times 10^6$ erg cm^{-2} s^{-1}. Possibly, it amounts to more, 1.4×10^7 erg cm^{-2} s^{-1} according to Anderson & Athay (1989). I thus estimate the radiative losses from the chromosphere of an average plage to $2 \ldots 4 \times 10^7$ erg cm^{-2} s^{-1}.

The reader is referred to Ulmschneider et al. (1991) and Narain & Ulmschneider (1996) for extensive discussions of chromospheric (and coronal) heating mechanisms. Ulmschneider and his group favour the dissipation of magneto-acoustic body waves (e.g. Fawzy et al. 2002). These authors had performed numerous simulations of chromospheric heating by acoustic waves and longitudinal tube waves. Transversal tube waves play apparently a minor role. The wave flux generated in the convection zone was calculated and found on the order of 10^9 erg cm^{-2} s^{-1}. The authors could explain the chromospheric emission of late-type stars and its dependence on effective temperature, surface gravity, metalicity, and on the filling factor which determines the coverage of the stellar surface with magnetic fields. The periods of the generated waves range from 300 s down to 5 s. The authors reason that short periods are required for heating, since strong gradients in shocks are needed.

However, strong lateral structuring represents another topology with strong gradients. Ryutova et al. (1991) treated tightly settled bundles of magnetic flux tubes with large inhomogeneities of the parameters, field strength, density, and temperature. These authors show These authors show that the propagation properties (shock formation, dissipation) change strongly strongly compared to the case of isolated tubes. Yet, Ryutova et al. (1991) treat waves running perpendicularly to the magnetic field. I do not know of similar work with waves along the field.

A heating mechanism caused by relatively slow gas flows is the reorganisation of magnetic fields which become 'braided' by random motions at their rooting in the photosphere (van Ballegooijen 1986). The field inhomogeneities are re-distributed to small scales and their energy content is dissipated in field-aligned electric currents. Many analytical studies as well as numerical simulations have been performed since the work of van Ballegooijen (1986) in this direction, but mainly with application to coronal heating processes.

Finally, emergence of magnetic flux and fast reconnection have to be mentioned. This process releases magnetic energy, e.g., in flares, and possibly in moustaches.

4. Conclusions

Two topics were treated in this review, the chromosphere of sunspot umbrae and the chromosphere of plages. I tried to start with *Old Wisdom* and to come to *New Insight*. The review is certainly incomplete, I apologise to those whose work was not properly acknowledged. I had learned long ago that new insight requires hard work and patience, and that it always raises new questions. Among the unsolved problems, which have been with us since many years, remain the chromospheric heating mechanisms. Yet the future for observational improvement with new facilities and for the understanding with the developments of educated theoretical simulations appears prosperous.

Georg Christoph Lichtenberg (*1742; †1799), professor for physics in Göttingen, modifies a citation from Shakespeare's Hamlet:

... have said, there exist many things in heaven and earth of which nothing is contained in our compendiis. ... One may reply confidently: Well, but instead many things are contained in our compendiis of which neither in heaven nor on earth anything exists.

This stimulates oneself to diligent writing.

Acknowledgements. I thank my collaborators for their help and T. Felipe García et al. as well as H. Schleicher for supplying figures for this contribution. This work was supported by Deutsche Forschungsgemeinschaft through grant KN 152/29-4.

References

Abdelatif, T., Lites, B. W., & Thomas, J. H. 1983, BAAS, 15, 719

Al, N., Bendlin, C., Hirzberger, J., Kneer, F., & Trujillo Bueno, J. 2004, A&A, 418, 1131

Anderson, L. S., & Athay, R. G. 1989, ApJ, 346, 1010

Beckers, J. M. 1964, A Study of the Fine Structures in the Solar Chromosphere (AFCRL Environmental Research Paper No. 49, PhD thesis Utrecht University)

Beckers, J. M., & Tallant, P. E. 1969, Sol. Phys., 7, 351

Beebe, H. A., Baggett, W. E., & Yun, H. S. 1982, Sol. Phys., 79, 31

Bello González, N., & Kneer, F. 2008, A&A, 480, 265

Berlicki, A., & Heinzel, P. 2010, MmSAI, this volume

Bruzek, A. 1967, Sol. Phys., 2, 451

Cannon, C. J. 1970, ApJ, 161, 255

Centeno, R., Socas-Navarro, H., Collados, M., & Trujillo Bueno, J. 2005, ApJ, 635, 670
Denker, C. 1996, PhD thesis, Göttingen
Ellerman, F. 1917, ApJ, 46, 298
Fabiani Bendicho, P., Kneer, F., & Trujillo Bueno, J. 1992, A&A, 264, 229
Fawzy, D., Stępień, K., Ulmschneider, P., Rammacher, W., & Musielak, Z. E. 2002, A&A, 386, 994
Felipe, T., Khomenko, E., Collados, M., & Beck, C. 2008, 12th ESP Meeting, Freiburg, Germany, Online at http://espm.kis.uni-freiburg.de
Fontenla, J. M., Avrett, E. H., & Loeser, R. 1993, ApJ, 406, 319
Giovanelli, R. G. 1972, Sol. Phys., 27, 71
Hammer, R. 1982, ApJ, 259, 779
Hansteen, V. H., Carlsson, M., & De Pontieu, B. 2010, MmSAI, this volume
Khomenko, E., & Collados, M. 2006, ApJ, 653, 739
Kneer, F., & Mattig, W. 1978, A&A, 65, 17
Leenaarts, J., Carlsson, M., Hansteen, V. H., & Rouppe van der Voort, L. H. M. 2010, MmSAI, this volume
Linsky, J. L., Worden, S. P., McClintock, W., & Robertson, R. M. 1979, ApJS, 41, 47
Lites, B. W., & Skumanich, A. 1982, ApJS, 49, 293
Martínez Pillet, V., Lites, B. W., & Skumanich, A. 1997, ApJ, 474, 810
Mattig, W., & Kneer, F. 1981, A&A, 93, 20
Mihalas, D. 1970, in Stellar Atmospheres, 1st edition (Freeman, San Francisco)
Musman, S. 1965, AJ, 70, 145
Narain, U., & Ulmschneider, P. 1996, Space Sci. Rev., 75, 453
Neckel, H. 1999, Sol. Phys., 184, 421
Pariat, E., Schmieder, B., Berlicki, A., et al. 2007, A&A, 473, 279
Poland, A., Skumanich, A., Athay, R. G., & Tandberg-Hanssen, E. 1971, Sol. Phys., 18, 391
Qiu, J., Ding, M. D., Wang, H., Denker, C., & Goode, P. R. 2000, ApJ, 544, L157
Ryutova, M., Kaisig, M., & Tajima, T. 1991, ApJ, 380, 268
Sánchez-Andrade Nuño, B., Bello González, N., Blanco Rodríguez, J., Kneer, F., & Puschmann, K. G. 2008, A&A, 486, 577
Scheuer, M. A., & Thomas, J. H. 1981, Sol. Phys., 71, 21
Schrijver, C. J., & Harvey, K. L. 1989, ApJ, 342, 481
Schrijver, C. J., Coté J., Zwaan, C., & Saar, S. H. 1989, ApJ, 337, 964
Severny, A. B. 1956, Observatory, 76, 241
Shine, R. A., & Linsky, J. L. 1972, Sol. Phys., 25, 357
Socas-Navarro, H., Trujillo Bueno, J., & Ruiz Cobo, B. 2000, Sci, 288, 1396
Socas-Navarro, H., McIntosh, S. W., Centeno, R., de Wijn, A. G., & Lites, B. W. 2009, ApJ, 696, 1683
Spruit, H. C. 1982, Sol. Phys., 75, 3
Thomas, R. N. 1965, in Some Aspects of Non-Equilibrium Thermodynamics in the Presence of a Radiation Field (University of Colorado Press, Boulder)
Turova, I. P., & Grigoryeva, S. A. 2000, Sol. Phys., 197, 43
Turova, I. P., Teplitskaja, R. B., & Kuklin, G. V. 1983, Sol. Phys., 87, 7
Tziotziou, K. 2007, in The Physics of Chromospheric Plasmas, ed. P. Heinzel, I. Dorotovič, & R. J. Rutten, ASPCS, 368, 217
Uchida, Y., & Sakurai, T. 1975, PASJ, 27, 259
Ulmschneider, P., Priest, E. R., Rosner, R., 1991, in Mechanisms of Chromospheric and Coronal Heating (Springer, Berlin)
van Ballegooijen, A. A. 1986, ApJ, 311, 1001
van Noort, M. J., & Rouppe van der Voort, L. H. M. 2006, ApJ, 648, L73
Vernazza, J. E., Avrett, E. H., & Loeser, R. 1981, ApJS, 45, 635
Wenzler, T., Solanki, S. K., & Krivova, N. A. 2005, A&A, 432, 1057
Wittmann, A. 1969, Sol. Phys., 7, 366
Zhugzhda, Y. D., Staude, J., & Locans, V. 1983, Pub. Debrecen Heliosph. Obs., 5, 451